An Investigation of the Coefficient of Variation Using the Colored Stochastic Hodgkin-Huxley Equations

Najdavan A. Kako

Submitted to the
Institute of Graduate Studies and Research
in partial fulfillment of the requirements for the Degree of

Master of Science
in
Computer Engineering

Eastern Mediterranean University
June 2013
Gazimağusa, North Cyprus

Approval of the Institute of Graduate Studies and Research

Prof. Dr. Elvan Yılmaz
Director

I certify that this thesis satisfies the requirements as a thesis for the degree of Master of Science in Computer Engineering.

Assoc. Prof. Dr. Muhammed Salamah
Chair, Department of Computer Engineering

We certify that we have read this thesis and that in our opinion it is fully adequate in scope and quality as a thesis for the degree of Master of Science in Computer Engineering.

Prof. Dr. Marifi Güler
Supervisor

Examining Committee

1. Prof. Dr. Erden Başar
2. Prof. Dr. Marifi Güler
3. Assoc. Prof. Dr. Ahmet Ünveren

ABSTRACT

In recent years, it has been argued and experimentally shown that ion channel noise in neurons can have profound effects on the neuron’s dynamical behavior. Most profoundly, ion channel noise was seen to be able to cause spontaneous firing and stochastic resonance.

It was recently found by (Güler, 2011) that a non-trivially persistent cross correlation takes place between the transmembrane voltage fluctuations and the component of open channel fluctuations attributed to the gate multiplicity. This non-trivial phenomenon was found to play a major augmentative role for the elevation of excitability and spontaneous firing in the small size cell. In addition, the same phenomenon was found to significantly enhance the spike coherence. More recently, Fox and Lu’s stochastic Hodgkin-Huxley equations were extended by incorporating colored noise terms into the conductances therein, to obtain formalism capable of capturing the addressed cross correlations (Güler, 2013).

In this thesis, statistics of the coefficient of variation, obtained from the colored stochastic Hodgkin-Huxley equations, was studied. Our investigation reveals that the colored noise term enhances the agreement with the microscopic simulation results.

Keywords: Colored Noise, Channel Noise, Stochastic Ion Channel, Small Size Membrane, Stochastic Hodgkin-Huxley Equations

ÖZ

Son yıllarda, nöronlardaki ion kanal gürültüsünün nöron dinamiği üzerinde hayati etki yapabildiği deneysel olarak da kanıtlanmıştır. Bu kapsamda, kendi kendine ateşleme ve stokastik rezonans en çarpıcı bulgulardır.

İyon kanallarında çoklu geçit bulunmasının, voltage dalgalanmaları ve açık kanal dalgalanmaları arasında ilk bakışta gözükmeyen bir daimi çapraz ilişkiye neden olduğu (Güler, 2011) ortaya çıkartılmıştır. Bu ilk bakışta gözükmeyen olgunun, küçük boyutlu hücrelerde yüksek uyarılma ve kendi kendine ateşlemeye neden olduğu bulunmuştur. Daha yakın zamanda, Fox ve Lu’nun stokastik Hodgkin-Huxley denklemleri geçirgenliklere renkli gürültü terimleri ekleyerek genişletilmiştir (Güler, 2013)

Bu tezde, yukarıdaki model renklendirilmiş stokastik Hodgkin-Huxley denklemleri kullanılarak varyasyon katsayısı istatistiği incelenmiştir. Renkli gürültü terimlerinin mikroskopik benzeşim sonuçlarıyla uyumu arttırdığı gözlenmiştir.

Anahtar Kelimeler: Renkli Gürültü, Kanal Gürültüsü, Stokastik Iyon Kanalları, Küçük Boyutlu Zar, Stokastik Hodgkin-Huxley Denklemleri

Many Hands Make Light Work

***I Dedicate this Thesis to my Parents, my Family and my Friends*.**

ACKNOWLEDGMENT

I would like to express my gratitude for my supervisor Prof. Dr. Marifi Güler for his knowledge, guidance, and effort without which this research would not have been possible.

I thank a lot to my family who supported me all throughout my studies. This study is dedicated to them as an indication of their significant support during this study as well as my life.

TABLE OF CONTENTS

LIST OF TABLES

LIST OF FIGURES

Chapter 1

INTRODUCTION

Neurons show that electrical activity is under the effect of the noise of external and internal types (Faisal A. S., 2008). External noise originates from synaptic signal transmission, while internal noise is particular to the cell. This is the main source of internal noise because there is a limitable number of a voltage-gated ion channel in the neural membrane patch. In cell membrane, these ion channels are water filled holes that are formed by proteins embedded in the lipid bilayer, add-on that each type of ion channel is free to select a particular kind of ion (Hille, 2001). They play a primal physiologic role to spark cells through conductance for potassium and sodium which is eased by voltage-gated ion channels. These channels have two states; open or close. The number of open channels fluctuates in apparently random style (Sakmann, 1995) which indicates fluctuation in conducting membrane which in turn refers to fluctuation in transmembrane voltage. The membrane area is very large when the number of ion channels is big, dynamic voltage is presented by the famed Hodgkin-Huxley (Hodgkin, 1952) equations. When the membrane patches are small, anyway, the effect of conductance fluctuation on cells voltage activity is truly deep and not-trivial. Stochasticity of the single open channels directly affects the spike pattern and these suggested by experimental investigation ((Sigworth, 1980); (Lynch, 1989); (Johansson, 1994)) which cause spontaneous firing are the noise on that ion channel ((Koch, 1999);

(White, Klink, Alonso, & Kay, 1998)). Results of patch-clamp experiments in outside cell body have shown that channel noise is in the soma and dendrites generate voltage change-down that is big enough to make difference on timing, initiation, and propagation of action potentials ((Diba, 2004); (Jacobson, 2005); (Dorval, 2005); (Kole, 2006)). Stochastic resonance is the phenomenon noticed to happen in a system of voltage-dependent ion channel in the form of peptide alamethicin (Bezrukov, 1995). Gating ion channel typically formed, without referring to partial details by Markovian methods moving between open-close states for every single gate making channel. Markov operation applies autonomicly on each gate due to no collaboration between gates. The whole gates in a channel must be open for the opening the channel. We mean thereby four n-gated in potassium channel, three m-gates and one h-gate in sodium.

In small neural membrane patches, spontaneous activity phenomenon occurs (in the case of repeating spikes or bursts) and the reason about that is the internal noise from ion channels. These phenomenon proven through numerical simulations of channel dynamics and theoretical investigations ((DeFelice, 1992); (Strassberg, 1993); (Lu, 1994); (Chow, 1996); (Rowat, 2004); (Güler, 2007); (Güler, 2008); (Güler, 2011) (Güler, 2013)); besides, those experiments have shown the happening of stochastic resonance and the coherence of the procreated spike trains ((Jung, 2001); (Schmid G. G., 2001); (Özer, 2006)). Even when the numbers of ion channels are large, channel fluctuations might become critical near to the action potential threshold ((Schneidman, 1998); (Rubinstein, 1995)); the small number of ion channels that are open at the action potential threshold can influence the accuracy of timing of action potential. Also it has been clarified that ion channel noise affects the spike generation in axons ((Faisal A. A., 2007); (Ochab-Marcinek, 2009)).

1.1 Scope and Organization

In this thesis, statistics of the coefficient of variation, to be obtained from the colored stochastic Hodgkin-Huxley equations, will be studied with results. The thesis is organized as follows. Chapter 1 will be an introduction. Chapter 2 illustrates neuron structure and morphology, the Hodgkin Huxley equation will be described in chapter 3, chapter 4 contains the membrane dynamics which is described by (Güler, 2013), chapter 5 includes the spike coherence and chapter 6 involves the experiments and results.

Chapter 2

NEURONS

2.1 Morphology and Structure

In the brain science, the most important concept is the concept of the neuron. They are highly specialized cells for producing electrical signals in react chemical and other inputs, and propagating them to other neurons. These cells have a special type of morphology like axon and dendrite. The function of dendrites is to receive input signals from other cells and transmit it to soma (main body of neuron). The neuronal output is carried to other cells by axon. The embranchments structure of the dendritic tree raises surface district of the cell bettering the ability of neuron to take inputs from another neuron through synaptic connections. Information flow in a neuron is shown in Figure 1. In single neuron, the axon length can extend to pass a large part or whole body cell. It has been estimated that cortical neurons in mouse brain, transmit out totally about 40 mm of axon and in their branched dendritic tree, it has been shown that they have approximately about 4 mm average of 180 synaptic connection with another cells per µm whilst this tree receives two synaptic on average per µm in length. The cell body (soma) of cortical neuron amounts in diameter from 10 to 50 µm (Abbott & Dayan, 2002).

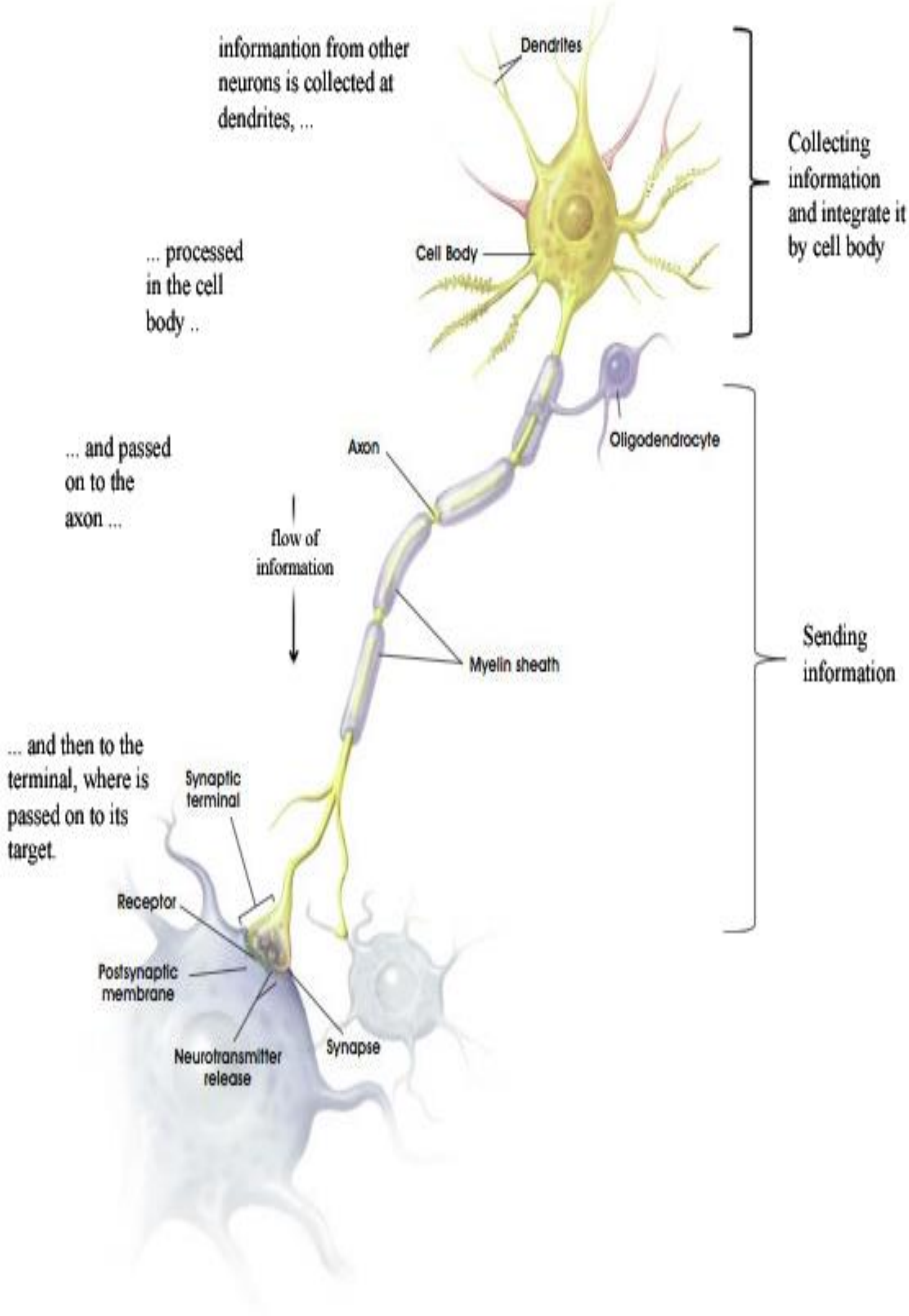

Figure 1: Information Flow in a Neuron (Whishaw, 2009)

2.1.1 What is a Spike?

Spikes are the major method of communications between the neurons. Every neuron received a spike from 10,000 through the synapse on its dendritic tree. The membrane potential is changed by electrical transmembrane currents produced by neuron inputs. Synaptic currents generate inflections, called postsynaptic potentials (PSPs). Large currents are significant more than small current because they produce significant PSPs that can be amplified by the voltage-sensitive channels applied in the neuronal membrane and indicate to the generation of an action potential (spike) (Izhikevich, 2007).

2.1.2 Membrane Proteins

The cell membrane has large proteins through which the materials can flow. To understand the functions of neuron, it is useful to know how the membrane protein work and how these proteins assist in transporting the substances through membrane. We classify it into three groups. For each case, the protein's function has an appropriate shape or ability to change its shape according to its function. The groups are channels, gates and pumps.

2.1.2.1 Channels

The channel or holes is one of some membrane protein shapes created to help substances across it. Variation of protein and holes size allow different materials to access and exit the neuron what works as channels are protein molecules for first class sodium (Na+), potassium (K+), calcium (Ca2+), and chloride (Cl-).

2.1.2.2 Gates

The ability to change shape is one of some protein molecules features. These shapes serve as gates when other chemicals connect to them. In these cases, the protein molecules work as door lock. When a key found in an appropriated inserted shape the locking device changes form and become activated. There are some other cases where gates change their shape according to certain conditions in their environment, such as electrical charge or temperature change.

2.1.2.3 Pump

Another change in protein molecules to act as pumps, substances needs energy to move through membrane transporter. For example, there is a protein that changes its form to pump Na+ ions and K+ ions in two different directions. Add-on protein pump transports many substances.

2.1.3 Synapse

The shape that has been jointed between two successive cells is called synapse which provides a way to transmit the information to other neuron when the axon of afferent neuron is connected to efferent one. Axon finishes at synapse, ion channels opening to generate influx of ca2+ that induct to release the neurotransmitter if the voltage transient of action potential. At the postsynapse side or when the signal is received, the neurotransmitter joins to receptors making ion-conducting channels to open. The synapse can have either an excitatory, depolarized, or an inhibitory, typically hyperpolarizing, effect on the postsynaptic neuron (Abbott & Dayan, 2002).

Synapses are distributed by specified pattern over dendritic tree. Inhibitory synapses are closer than excitatory generally, although those two synapses are also at far dendritic areas and, exist on some spines in joining with excitatory input (Segev I., 2003). In appointed area from dendritic tree that input source is mapped on their tree discriminatorily as in this systems such as pyramidal hippocampal cells and cerebellar purkinje (Haberly L. B., 1990), it's better if the distribution on dendritic surface randomly.

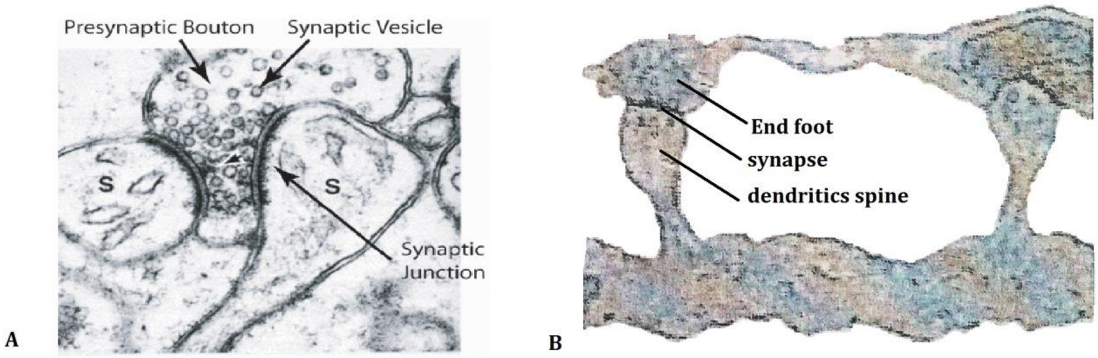

Figure 2: Tow Electronic Micrographic Picture of Synapse in Real Neurons

a) Electron micrograph of recitative spiny synapses (s) designed on the dendrites of rodent hippocampal pyramidal cell.
b) An electron micrograph picture catches the synapse design where the terminal button of one neuron connects with a dendritic spine on a dendrite of second neuron. (Whishaw, 2012).

2.2 Electrical Activity of Neuron and Membrane Potential

The difference between the inside of neuron and the environment of extracellular liquid in electrical potential is called a membrane potential. In state of resting, the action potential interior neuron membrane gets to $-70\,mV$. However, this action potential is assumed conventionally to be $0\,mV$ for more fitness and also to consider the cell is polarized in this situation. The potential is seen as an equilibrium point between the influx of ions to inside neuron and outside of cell. The difference generated by this potential is kept by ion pump existing in the membrane preserving concentration gradients. For instance, the concentration of Na+ outside the cell is much more than inside it, and K+ is highly concentrated intracellular than outside cell fluid. Accordingly, in the case of cell transition the ions influx to interior and exterior of cell influenced by both voltage and concentration gradients. Hyperpolarization is a process of positive charged ion current influx outside of neuron (or negative charged ion current influx inside of neuron) within open channels to make membrane potential much negative, and depolarization is an influx of current to inside cell to make the membrane potential less negative or positive. A positive feedback starts, when the depolarization of a cell is large enough to boost the membrane potential overhead threshold level, and leads the neuron to produce an action potential. In electrical potential, the action potential approximates to $100\,mV$ through the cell membrane that persists for around $1ms$. At one occasion, an action potential to happen may not begin another spike as soon as the previous one ends and this period is named absolute refractory. The most important feature of action potential that unwanted sub-threshold fluctuation could be reduced over space mostly $1\,mm$ and they can spread over large space without easement along axon operation

(Abbott & Dayan, 2002). Figure 3 describes dynamic voltage of a neuron cell through an action potential; however, it is synthesized by conformable ion channel during an action potential. The Figure represents the rest potential in real value $-70\ mV$.

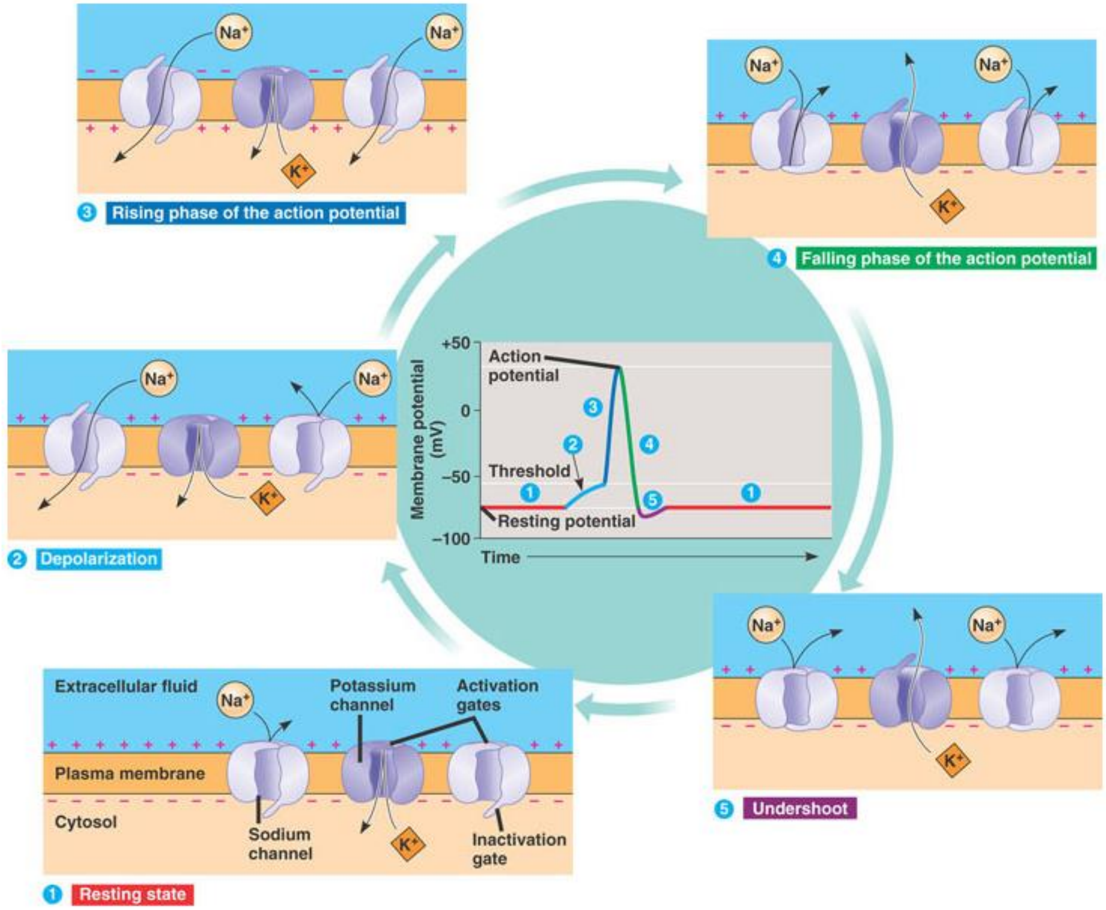

Figure 3: Phase of Action Potential (Whishaw, 2012)

Chapter 3

HODGKIN HUXLEY APPROACH

During the last decades, many neural models have been found and developed for different needs. The difference of these models depends on the structure of realistic biophysical model. The most significant of these models which depends on many experiment investigations through long time is the Hodgkin Huxley model, and the one that this thesis focuses on the color noise model which was set by (Güler, 2013), which is extension of Hodgkin-Huxley model to small size membranes. Different models may be needed in different studies relying on biological properties of models, complexity and the implementation cost. In (1952) Hodgkin and Huxley have been attached as landmark with the modeling method of neural excitability. The chapter briefly explains Hodgkin – Huxley model.

3.1 The Hodgkin-Huxley Model

By using space and voltage clamps techniques depending on experimental investigation on giant squid axon, it was shown by Hodgkin-Huxley (1952) that two prime ionic components where from the current fluxing through the squid axon membrane, which are I_{na} and I_k (sodium and potassium channels on a par with components) these currents are powerfully affected via membrane potential V_m.

As a result of their observation, a mathematical model has been developed to make a significant model based on which many realistic neural models have been developed.

In HH model, specifically a part of nerve membrane which is carried by electrical properties can be modeled via an adequate circuit in which current influx through the membrane with two prime components, the first one joined with the membrane capacity charge and the other one joined with the activity of specific kinds of ion through the membrane. The ionic current is further sub split into three distinguishable components, the current of sodium I_{na}, potassium I_k, and a little leakage current I_l that is primarily carried by chloride ions.

The differential equation corresponding to the electrical circuit is as follows:

$$C_m \frac{dV_m}{dt} + I_{ion} = I_{ext} \tag{1}$$

where C_m is membrane capacitance, V_m is membrane potential, I_{ext} is an external current and I_{ion} is the ionic current fluxing through the membrane and can be obtained from these equations:

$$I_{ion} = \sum_i I_i \tag{2}$$

$$I_i = g_i(V_m - E_i) \tag{3}$$

where I_i is represents every ionic component having a joined conductance g_i and reversal potential E_i.

The three I_i terms in the squid giant axon model are: sodium current I_{Na}, potassium current I_K and a small leakage current I_l and the equation that represents those three currents is:

$$I_{ion} = I_{Na} + I_K + I_L = g_{Na}(V_m - E_{na}) + g_K(V_m - E_K) + g_L(V_m - E_L \tag{4}$$

The combined influence of many number of microscopic ion channels in the membrane originates the microscopic $g_i(g_L, g_K, g_{Na})$ conductance. Ion channel may contain a small number of physical gates that organize ion influx within the channel. Ions can go across channel when all of the gates are in the permissive state while the channel is open.

3.1.1 The Ionic Conductances

In permissive state, all of the gates for a specific channel ion can go within a channel while the channel is open. The potassium and sodium conductances empirically described by the formal assumption, which is attained by voltage clamp experiments are:

$$g_k = \bar{g}_k n^4 , \tag{5}$$

$$g_{na} = \bar{g}_{na} m^3 h , \tag{6}$$

where

$\left.\begin{matrix} n \\ m \\ h \end{matrix}\right\}$ are ion channel gate variables dynamics

$\bar{g}_i$ is a constant with the dimensions of conductance per cm^2 (mention that n between 0 and 1) . In order to normalize the result, a maximum value of conductance $\bar{g}_i$ is required.

n , m and h dynamically are as follows:

$$\dot{n} = \frac{dn}{dt} = \alpha_n(1-n) - \beta_n n \tag{7}$$

$$\dot{m} = \frac{dn}{dt} = \alpha_m(1-m) - \beta_m m \tag{8}$$

$$\dot{h} = \frac{dh}{dt} = \alpha_h(1 - h) - \beta_h h \tag{9}$$

where

$\left.\begin{array}{l}\alpha_x\\ \beta_x\end{array}\right\}$ are gating functions (vary with voltage but not with time)

n is a dimensionless variable (varies between 0 and 1), add-on, represents the probability of a single gate being in the permissive state.

The membrane potential begins in resting state in voltage clamp ($V_m = 0$) and is then instantly finished when a new voltage clamp ($V_m = V_c$) starts. The calculation of equations (7), (8) and (9) is a simple exponential of the format:

$$x(t) = x_\infty(v_c) - \left(x_\infty(v_c) - x_\infty(0)\right)exp(-t/\tau_x) \tag{10}$$

$$x_\infty(0) = \alpha_x\ (0)/\alpha_x\ (0)\ +\ \beta_x(0) \tag{11}$$

$$x_\infty(v_c) = \alpha_x\ (v_c)/\alpha_x\ (v_c)\ +\ \beta_x(v_c) \tag{12}$$

$$\tau_x(v_c) = [\alpha_x\ (v_c) + \beta_x\ (v_c)]^{-1} \tag{13}$$

where

x indicates time basing on gate variables n, m and h

$\left.\begin{matrix} x_\infty(0) \\ x_\infty(v_c) \end{matrix}\right\}$ are the value of gating variable at conventional resting state

$\tau_x(v_c)$ clamp voltage indicates the constant time course for approaching the steady state value of $x_\infty(v_c)$ when the voltage is clamped to v_c.

Hodgkin and Huxley calculated constant α_i, β_i as functions of V in the following format:

$$\alpha_i = \frac{x_\infty(V)}{\tau_n(V)} \tag{14}$$

$$\beta_i = \frac{1 - x_\infty(V)}{\tau_n(V)} \tag{15}$$

i represents for n, m and h ion channel gate variables

The equations below are the expressions rate constants α_i and β_i that are based on the experience known as:

$$\alpha_n(v) = 0.01 \, \frac{10 - v}{exp\left(\frac{10 - v}{10}\right) - 1}, \tag{16}$$

$$\beta_n(v) = 0.125 \, exp\left(\frac{-v}{80}\right), \tag{17}$$

$$\alpha_m(v) = 0.1 \, \frac{25 - v}{exp\left(\frac{25 - v}{10}\right) - 1}, \tag{18}$$

$$\beta_m(v) = 4 \, exp\left(\frac{-v}{18}\right), \tag{19}$$

$$\alpha_m(v) = 0.07\, exp\left(\frac{-v}{20}\right), \tag{20}$$

$$\beta_h(v) = \frac{1}{exp\left(\frac{30-v}{10}\right)+1}, \tag{21}$$

where $\alpha_i(v)$ and $\beta_i(v)$ are the transition rates between open and closed states of the channels.

Chapter 4

DYNAMICS OF THE LIMITED SIZE MEMBRANES

This differential equation determines the evaluation of the transmembrane voltage V in time

$$C\ \frac{dV}{dt} = -g_K(V_m - E_K) - g_{Na}(V_m - E_{na}) - g_L(V_m - E_L) + I \qquad (22)$$

where ψ_K and ψ_{Na} are dynamic channel variables. ψ_K corresponds to the proportion of open potassium channels to the total number of potassium channels in the membrane; similarly, ψ_{Na} denotes the proportion of open sodium channels. There exist four n-gates in a potassium channel, and three m-gates and one h-gate in a sodium channel. A channel is open when all its gates are open; otherwise, it is closed. In the limit of infinite membrane size, the channel variables attain their deterministic HH values, that is, $\psi_K = n^4$ and $\psi_{Na} = m^3h$, where $n, m,$ and h are the gating variables. For a membrane

Table 1: Constants of the Membrane.

$\boldsymbol{C}$	Membrane capacitance	1μF/cm^2
$\boldsymbol{g_K}$	Maximal potassium conductance	36mS/cm^2
$\boldsymbol{E_K}$	Potassium reversal potential	−12mV
$\boldsymbol{g_{Na}}$	Maximal sodium conductance	120mS/cm^2
$\boldsymbol{E_{na}}$	Sodium reversal potential	115mV
$\boldsymbol{g_L}$	Leakage conductance	0.3mS/cm^2
$\boldsymbol{E_L}$	Leakage reversal potential	10.6mV
	Density of potassium channels	18 chns/μm^2
	Density of sodium channels	60 chns/μm^2

that contains N_K potassium channels and N_{Na} sodium channels, the numbers of open n-gates, open m-gates, and open h-gates read in terms of the gating variables as $4N_K n$, $3N_{Na}m$, and $N_{Na}h$, correspondingly. The values of the constant membrane parameters used in equation (22) are provided in Table 1.

The dynamics of gates obeys the following Markov process. An n-gate that is closed at time t continues to remain closed at time $t + \Delta t$ with the probability given by $exp(-\alpha_n \Delta t)$. If the gate is open at time t, then the probability that it remains open at time $t + \Delta t$ is $exp(-\beta_n \Delta t)$. The voltage-dependent parameters α_n and β_n are opening and closing rates of n-gates. An analogous procedure applies to the m-gates and the h-gates. As we will see later, a microscopic simulation step, which executes these dynamics of gates and is then followed by keeping track of each channel state, can be approximated effectively by computing ψ_K and ψ_{Na} directly as the fractions of the open potassium and sodium channels, respectively. The rate functions read as follows:

$$\alpha_n = (0.1 - 0.01V)/(exp(1 - 0.1V) - 1), \tag{23a}$$

$$\beta_n = 0.125\, exp(-V/80), \tag{23b}$$

$$\alpha_m = (2.5 - 0.1V)/(exp(2.5 - 0.1V) - 1), \tag{23c}$$

$$\beta_m = 4\, exp(-V/18), \tag{23d}$$

$$\alpha_h = 0.07\, exp(-V/20), \tag{23e}$$

$$\beta_h = 1/(exp(3 - 0.1V) + 1). \tag{23f}$$

4.1 The Essence of NCCP [The Non-Trivial Cross Correlation Persistency]

Considering that the colored model was directly motivated by NCCP, it is helpful to emphasize the essentials of this phenomenon before turning to the study focus (For further details, (Güler, 2011)).

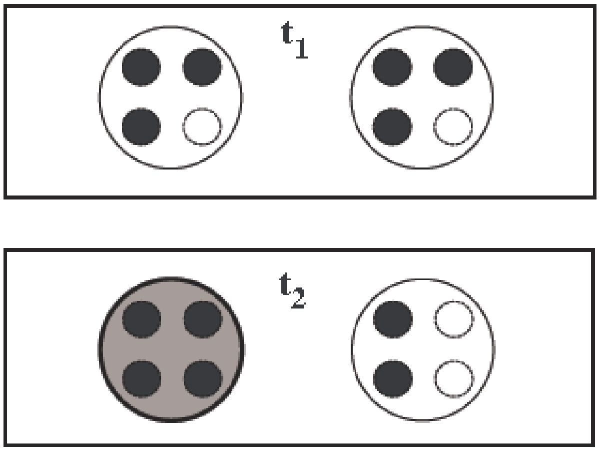

Figure 4: Depiction of Gate-to-Channel Uncertainty

Two possible conformational states of a toy membrane, comprising just two potassium channels, are shown at two different time's t_1 and t_2. Filled black dots and small circles represent open and closed gates, respectively. The bigger circles represent channels. Despite the numbers of open gates at t_1 and at t_2 being the same (six), one channel (shadowed) is open at t_2 while no channel is open at t_1. Adopted from (Güler, 2011).

Due to the presence of a multiple number of n-gates in individual potassium channels, knowing n does not suffice to specify ψ_K uniquely. In (Güler, 2013), the term gate-to-channel uncertainty is coined to describe this lack of uniqueness (see Figure 4); and the term gate noise to denote the random fluctuations in n. It was stated that the construct $\psi_K - [\psi_K]$ singles out the channel fluctuations that arise from gate-to-channel uncertainty. Here $[\cdot\cdot\cdot]$ designates averaging over the possible configurations of the membrane having $4N_K n$ open n-gates. Unless the membrane is extremely small, it holds that

$$[\psi_K] \approx n^4 \tag{24}$$

It was shown (Güler, 2013) that a non-trivial correlation takes place between the fluctuations of the construct $\psi_K - [\psi_K]$ and the fluctuations of V within the phase of sub-threshold activity. This is the phenomenon that NCCP refers to. A property, crucial for the occurrence of NCCP, is that the autocorrelation time of the construct $\psi_K - [\psi_K]$ is finite but not zero. It can be deduced from equation (22) that if $\psi_K - [\psi_K] > 0$ throughout some period of time, then a negative variation, relative to the case of having $\psi_K - [\psi_K] = 0$, takes place in V along that period. Similarly, if $\psi_K - [\psi_K] < 0$ throughout the period, then a positive variation in V takes place. Then, provided that the residence time of $\psi_K - [\psi_K]$ in the same algebraic sign is long enough, NCCP materializes. A pictorial explanation is provided in Figure 5. The construct that reveals the gate-to-channel uncertainty associated with the sodium channels is $\psi_{Na} - [\psi_{Na}]$. The configuration average of the proportion of open sodium channels $[\psi_{Na}]$, obeys

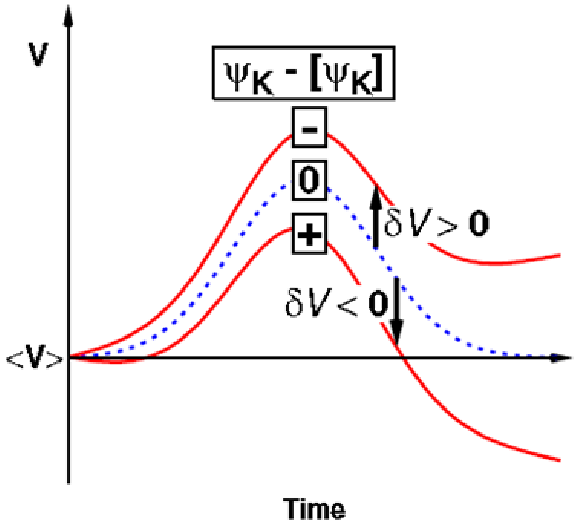

Figure 5: An Illustration of the Variation in the Voltage, Denoted by Δv, in Response to Deviations of the Construct $\Psi_k - [\Psi_k]$ from Zero (Adopted from (Güler, 2011))

$$[\psi_{Na}] \approx m^3 h \tag{25}$$

unless the membrane is extremely small.

4.2 Colored Formulation for the Conductances

Since the autocorrelation time of $\psi_K - [\psi_K]$ is not zero and the algebraic sign of it is durable (at a microscopic timescale), ψ_K reads as

$$\psi_K = [\psi_K] + Q_K, \tag{26}$$

where Q_K is a stochastic variable with zero expectation value at equilibrium and has some autocorrelation time greater than zero. Hence, the variable Q_K can be treated as colored noise. For the analytical implementation of NCCP, it suffices to elaborate Q_K.

It is more convenient to approximate equation (26) as

$$\psi_K = n^4 + \sigma_K q_K, \qquad (27)$$

where the approximation, equation (24), was utilized. Here q_K is a new stochastic variable; σ_K stands for the standard deviation of ψ_K, computed over the possible configurations of the membrane having $4N_K n$ open n-gates. It is, however, much easier to compute the standard deviation for the situation where every gate in each configuration is set to be open with the probability of n, without the constraint of being exactly $4N_K n$ open gates in each configuration. For the unconstrained situation, the following holds:

$$\sigma_K = \sqrt{\frac{n^4(1-n^4)}{N_K}}. \qquad (28)$$

In that derivation of σ_K, after taking the probability of a channel being open as n^4, the formulation of the random walk problem was employed. We assume that σ_K has given by equation (28) is a good approximation of the actual standard deviation, at least up to a proportionality constant absorbed into q_K. Note that σ_K vanishes in the limit of infinite membrane size, and therefore $\psi_K = n^4$ applies in that limit. When all the n-gates are open or closed, that is, when $n = 1$ or $n = 0$, there is no gate-to-channel uncertainty associated with the potassium channels, and therefore the colored noise term should vanish in these cases. It is indeed the situation in our formulation as σ_K becomes zero at these special values of n.

We take the stochastic variable q_K to obey the same type of equations as the position variable of a Brownian harmonic oscillator does. With this choice, q_K is stochastic, has memory, and demonstrates near periodicity, and its variance remains bounded. These are the properties that the construct $\psi_K - [\psi_K]$ with a nonzero autocorrelation time possesses. That is what lies behind our adoption of the Brownian harmonic oscillator as a biologically plausible emulator of the construct. The equations that describe the dynamics of q_K are specified accordingly as follows:

$$\tau\dot{q}_K = p_K, \tag{29a}$$

$$\tau\dot{p}_K = -\gamma_K p_K - \omega_K^2 D_n q_K + \xi_K, \tag{29b}$$

in which D_n is identical to

$$D_n \coloneqq \alpha_n(1-n) + \beta_n n \tag{30}$$

and ξ_k is a mean zero Gaussian white noise term with the mean square

$$\langle \xi_k(t)\xi_k(t') \rangle = \gamma_k T_k D_n \delta(t-t'). \tag{31}$$

The parameter τ corresponds to the unit time. The constants $-\gamma_k$, ω_K and $T_k -$ and the variables$-q_K$ and $p_K -$ are all in dimensionless units. D_n is a measure of how fast a conformational state loses memory (at a microscopic timescale). Note at this point that the transition probability of an n-gate from being closed to being open increases with αn, and the transition probability from being open to being closed increases with β_n. At larger values of D_n, q_K should switch sign at a faster average rate and exhibit more erratic behavior. Because of that, the constants ω_K and $\mathrm{T_k}$ (which are analogous to the angular frequency and the temperature, respectively) were accompanied by D_n. It is not a coincidence that the noise variance of the n-gates in the FL equations is likewise proportional to D_n. It follows from the non-equilibrium statistical mechanics (Zwanzig, 2001) that q_K, obeying the above equations, yields the following variance at equilibrium:

$$\langle \mathrm{q_k^2} \rangle_{\mathrm{eq}} = \frac{\mathrm{T_k}}{\omega_\mathrm{k}^2}. \qquad (32)$$

Note that the variance is a constant, as it should be.

It was stressed that like the construct $\psi_K - [\psi_K]$, the construct $\psi_{Na} - [\psi_{Na}]$ also has a finite but nonzero autocorrelation time, which induces NCCP attributed to the sodium channels. Then the colored formulation developed above for the potassium conductances can similarly be developed for the sodium conductances. Utilizing the approximation (25), we write ψ_{Na} analogous to equation (27) as:

$$\psi_{\mathrm{na}} = m^3 h + \sigma_{\mathrm{na}} \mathrm{q_{na}}, \qquad (33)$$

where q_{Na} is a stochastic variable with zero expectation value at equilibrium and some autocorrelation time greater than zero. σ_{Na} stands for the standard deviation of ψ_{Na}, computed over the possible configurations of the membrane having $3N_{Na}m$ open m-gates and $N_{Na}h$ open h-gates. The approach used for evaluating σ_K similarly applies for σ_{Na}, yielding

$$\sigma_{\mathrm{Na}} = \sqrt{\frac{\mathrm{m}^3(1-\mathrm{m}^3)}{\mathrm{N}_{\mathrm{Na}}}}\mathrm{h}. \tag{34}$$

In that evaluation, the channels were treated as if they do not accommodate h-gates, and then the obtained result was multiplied by h.

The stochastic variable q_{Na} obeys the same type of dynamical equations as q_K does,

$$\tau\dot{\mathrm{q}}_{\mathrm{Na}} = \mathrm{p}_{\mathrm{Na}}, \tag{35a}$$

$$\tau\dot{\mathrm{p}}_{\mathrm{Na}} = -\gamma_{\mathrm{Na}}\mathrm{p}_{\mathrm{Na}} - \omega_{\mathrm{Na}}^2\mathrm{D}_{\mathrm{m}}\mathrm{q}_{\mathrm{Na}} + \xi_{\mathrm{Na}}, \tag{35b}$$

in which D_{m} is identical to

$$\mathrm{D}_{\mathrm{m}} \coloneqq \alpha_{\mathrm{m}}(1-\mathrm{m}) + \beta_{\mathrm{m}}\mathrm{m} \tag{36}$$

and ξ_{k} is a mean zero Gaussian white noise term with the mean square

$$\langle\xi_{\mathrm{Na}}(\mathrm{t})\xi_{\mathrm{Na}}(\mathrm{t}')\rangle = \gamma_{\mathrm{Na}}\mathrm{T}_{\mathrm{Na}}\mathrm{D}_{\mathrm{m}}\delta(\mathrm{t}-\mathrm{t}'). \tag{37}$$

the variance q_{Na}, at equilibrium read as:

$$\langle\mathrm{q}_{\mathrm{Na}}^2\rangle_{\mathrm{eq}} = \frac{\mathrm{T}_{\mathrm{Na}}}{\omega_{\mathrm{Na}}^2}. \tag{38}$$

4.3 Implementing the Gate Noise

A complete set of analytical activity equations must capture not only NCCP but also the gate noise. In implementing the gate noise, we take FL’s Langevin equations for the gating variables as the reference point. But the white noise terms used in the equations have different noise variances in our case. The gating variables obey

$$\dot{n} = \alpha_n(1-n) - \beta_n n + \eta_n \tag{39a}$$

$$\dot{m} = \alpha_m(1-m) - \beta_m m + \eta_m \tag{39b}$$

$$\dot{h} = \alpha_h(1-h) - \beta_h h + \eta_h \tag{39c}$$

where we take the mean zero Gaussian white noise terms $\mathrm{n_n}$, $\mathrm{n_m}$, and $\mathrm{n_h}$ to have the mean squares

$$\langle \eta_n(t)\eta_n(t') \rangle = \frac{D_n}{4N_k}\,\delta(t-t') \tag{40a}$$

$$\langle \eta_m(t)\eta_m(t') \rangle = \frac{D_m}{3N_{Na}}\,\delta(t-t') \tag{40b}$$

$$\langle \eta_h(t)\eta_h(t') \rangle = \frac{D_h}{N_{na}}\,\delta(t-t') \tag{40c}$$

The terms D_n and D_m were defined in equations (31) and (37), respectively. D_h is defined likewise:

$$\mathrm{D_h} \coloneqq \alpha_\mathrm{h}(1-\mathrm{h}) + \beta_\mathrm{h}\mathrm{h} \tag{41}$$

The noise variances in the FL formulation differ from our variances in the following way. In the FL case, the variances of η_n and η_m are four and three times the variances given by equation (41a) and (41b), respectively. There is no difference in the variance of η_h between the two cases. FL employ a stochastic automaton model of the gates to derive master equations for potassium and sodium channels using four n-gates in a potassium channel and three m-gates and one h-gate in a sodium channel. In obtaining the stochastic version of the HH equations from the master equations, however, they considered the potassium channels to be made up of a single element of type n and the sodium channels to also be made up of a single element, but this time with two types, the m type and the h type. Following the derivation of the Langevin noise variances, they raised the channel variables to the appropriate powers, $\psi_K = n^4$ and $\psi_{Na} = m^3h$, for inclusion into the conductances. But for our gate noise computation, the number of gates matters, not the number of channels. Therefore, in obtaining equations (41a) and (41b), we have simply taken FL's variances and substituted N_K by $4N_K$ in the variance of η_n and substituted N_{Na} by $3N_{Na}$ in the variance of η_m.

4.4 The Complete Model

The following set of equations sums up the complete colored model that incorporates both NCCP and the gate noise:

$$C\dot{V} = -g_K\psi_k(V - E_K) - g_{Na}\psi_{Na}(V - E_{Na}) - g_L(V - E_L) + I, \tag{42a}$$

$$\psi_k = n^4 + \sqrt{\frac{n^4(1-n^4)}{N_k}}q_k, \tag{42b}$$

$$\psi_{Na} = m^3h + \sqrt{\frac{m^3(1-m^3)}{N_{Na}}}hq_{Na}, \tag{42c}$$

$$\tau\dot{q}_k = p_k, \tag{42d}$$

$$\tau\dot{q}_k = -\gamma_k p_k - \omega_k^2[\alpha_n(1-n) + \beta_n n]q_k\xi_k, \tag{42e}$$

$$\tau\dot{q}_{Na} = p_{Na}, \tag{42f}$$

$$\tau\dot{q}_{Na} = -\gamma_{Na}p_{Na} - \omega_{Na}^2[\alpha_m(1-m) + \beta_m m]q_{Na}\xi_{Na}, \tag{42g}$$

$$\dot{n} = \alpha_n(1-n) - \beta_n n + \eta_n, \tag{42h}$$

$$\dot{m} = \alpha_m(1-m) - \beta_m m + \eta_m, \tag{42i}$$

$$\dot{h} = \alpha_h(1-h) - \beta_h h + \eta_h, \tag{42j}$$

Table 2: Constant Parameters of the Model.

$\boldsymbol{\gamma_k = 10}$	$\boldsymbol{\omega_k^2}$=150	$\mathbf{T_k}$=400
$\boldsymbol{\gamma_{Na} = 10}$	ω_{Na}^2=200	T_k=800

where the Gaussian white noise terms have zero means and their mean squares obey

$$\langle \xi_k(t)\xi_k(t')\rangle = \gamma_k T_k[a_n(1-n)\beta_n n]\delta(t-t'), \tag{43a}$$

$$\langle \xi_{Na}(t)\xi_{Na}(t')\rangle = \gamma_{Na} T_{Na}[a_m(1-m)\beta_m m]\delta(t-t'), \tag{43b}$$

$$\langle \eta_n(t)\eta_n(t')\rangle = \frac{\alpha_n(1-n)+\beta_n n}{4N_k}\,\delta(t-t'), \tag{43c}$$

$$\langle \eta_m(t)\eta_m(t')\rangle = \frac{\alpha_m(1-m)+\beta_m m}{3N_{Na}}\,\delta(t-t'), \tag{43d}$$

$$\langle \eta_h(t)\eta_h(t')\rangle = \frac{\alpha_h(1-h)+\beta_h h}{N_{Na}}\,\delta(t-t'). \tag{43c}$$

Note that in the limit of infinite membrane size, the set of equations reduces to the HH equations. The constant model parameters are given in Table 2.

Chapter 5

SPIKE COHERENCE

5.1 Introduction

It is shown that what may affect firing threshold in neuron is not only the synaptic noise but also the randomness of the ion channel gating itself (Lecar & Nossal, 1971). Accordingly, channel noise which originates from stochastic nature of ion channel dynamics must be taken into account (Clay & DeFelice, 1983). Spiking and the spiking rate itself are affected by thus features as the threshold, (Skaugen & Walløe, 1979), the irregular noise-assisted improvement of transduction of external signals, such as, the phenomenon of stochastic resonance (Schmid G. G., 2004) and having a relationship with the efficiency for synchronization. (Schmid G. G., 2003) gives a name; but some like interesting phenomena. The source of the channel noise (White, Rubinstein, & Kay, Channel noise in neurons, 2000) is originally because of the oscillations of the mean number of open ion channels about the opposing mean values.

5.2 Spike Coherence

A sensitively regular measure of spike train is called coefficient of variation (CV), or the comparative difference of the interspike interval distribution. This regularity measure is given by,

$$CV := \frac{\sqrt{\langle \mathrm{T}^2 \rangle - \langle \mathrm{T} \rangle^2}}{\langle \mathrm{T} \rangle}. \tag{44}$$

$\langle \mathrm{T} \rangle$: The mean interspike interval $\langle \mathrm{T} \rangle = \lim_{N\to\infty} \frac{1}{N} \sum_i T_i$,

$\langle \mathrm{T}^2 \rangle$: The mean squared interval $\langle \mathrm{T}^2 \rangle := \lim_{\mathrm{N}\to\infty} \sum (\mathrm{t}_{\mathrm{i}+1} - \mathrm{t}_{\mathrm{i}})^2/\mathrm{N}$.

$CV = 1$ if the sequence of spikes, which corresponds to the Poissonian spike train, is discrete.

$CV < 1$ if the spike train is more ordered.

$CV = 0$ for a purely deterministic response.

The increasing system size $\mathcal{A}$ is against to the coefficient of variation. While the firing rate reduces monotonically with regard to the patch area, it has been proved that the coefficient of variation CV shows a discriminate minimum for an optimal patch size for which the spike train is mostly regular at same value. The phenomenon is called an intrinsic coherence resonance (Schmid G. G., 2001). At optimal dosage of internal noise, whose optimal size of the cell membrane patch approximately $\mathcal{A} = 1\mu\mathrm{m}^2$, the CV shows a minimum, where the spiking becomes prevalently more ordered. The external disturbances withstand by internal rhythm which is possessed through the spiking activity (Schmid G. H., 2007).

Chapter 6

RESULTS AND DISCUSSION

In this chapter, the coefficient of variation will be examined through sequence of experiments by comparing the colored noise model with the microscopic simulations. The microscopic simulations scheme represents the simple stochastic method (Zeng, 2004). The Markovian process is applied by this method to simulate each individual gate and go on for the rest of the gates. The input current in my simulation was changed to obtain the coefficient of variation for this investigation.

The aim of this is to see the effect of the cross-correlation persistency placed in the trans-membrane voltage fluctuation by adding the colored noise terms (Güler, 2013) into the conductance of the stochastic Hodgkin Huxley equations. Series of experiments were used to assess the colored noise model effectiveness, in a comparative manner with the Microscopic simulation as mentioned before (Zeng, 2004); by firstly running the experiments without include the colored noise model into the stochastic of the Hodgkin Huxley equations, and secondly running again the experiments with the same parameters but at this time, the colored noise model is included in the stochastic of the HH equations. By changing the variable (input current) for investigation purpose and measure the coefficient of variation, comparing with the microscopic simulation (as a reference).

In Figures (6, 7, 8, 9 and 10), we can see the effect of the NCCP on the Stochastic Hodgkin-Huxley equations with colored noise that enhance the coherence in the spike trains. It can be seen that when the input current is mostly low around $(1 - 3\ \mu A)$ the coefficient of variation that measured from the experiments when the colored noise model not included in the stochastic of the HH equation (without colored noise) in comparing with the Microscopic simulation is far from each other for small membrane size. But when the colored noise model is implied in the stochastic HH, the response will be more close to without colored term and microscopic simulation. Since, that is what the colored noise model effects on. It is clear in Figure 10. In Figure 11 I have collected the coefficient of variation of the HH for both (without colored noise and with colored noise) to the values of experiments of a certain size and subtract the first of the second and took the value of this size to represent in the recent Figure, and so on for the other sizes. The aim of this phenomenon is to show that the greater size of the membrane, the lower coefficient of variation. In Figures (6, 12 and 13) we fixed the number of sodium channels and increase the number of potassium channel and in Figures (7, 14 and 15) we fixed the number of potassium channels and increase the number of sodium channels, to see the effect of colored noise on the membrane through the effectiveness of potassium and sodium by increasing the number of channels of first and keep the second steady and vice versa, thorough experiments it appeared that the colored noise depend on membrane size whatever was the number of potassium and sodium channels. In small membrane size the colored noise enhance the coherence of spike and agreement with microscopic simulation. In other words, the value of colored noise becomes very close with the without colored noise by increasing the size of the cell membrane.

6.1 Technologies Used

The model equations (35, 36) was numerically developed and solved through computer program by Güler. In the simulation, the input current was a time autonomous which was modified so that the program could process time dependent current. By using C++ programming language the model was developed and for plotting the result MATLAB was used.

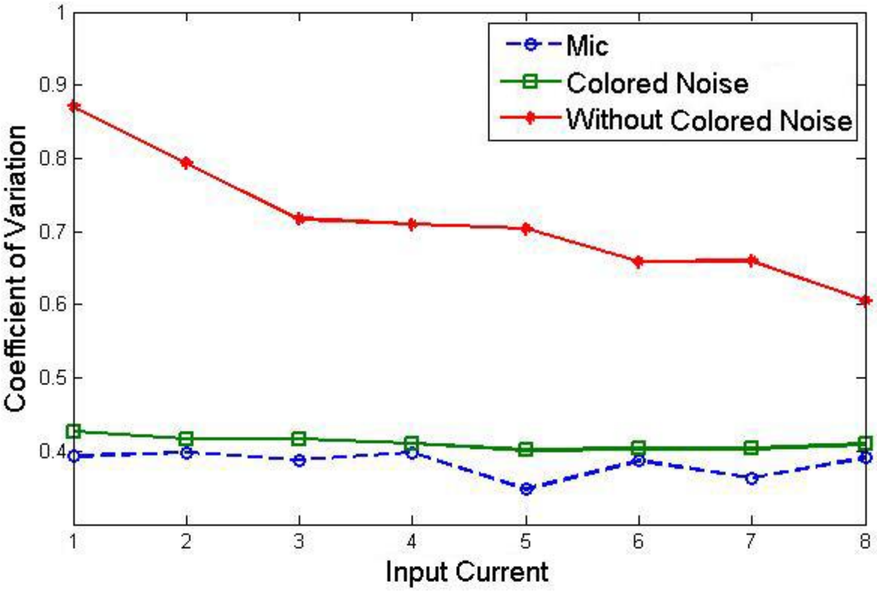

Figure 6: Coefficient of Variation for a Membrane of 300 Potassium and 1000 Sodium Channels. A 5 Sec. Time Was Used

The coefficient of variation against the input current, the three plots shown correspond to colored noise term, the microscopic simulations, and the without colored noise. When the colored noise it included to the stochastic HH the neural work enhanced and the result are close to the microscopic simulation result where the without colored noise is so far. The coherence for colored noise is much better than the without colored noise.

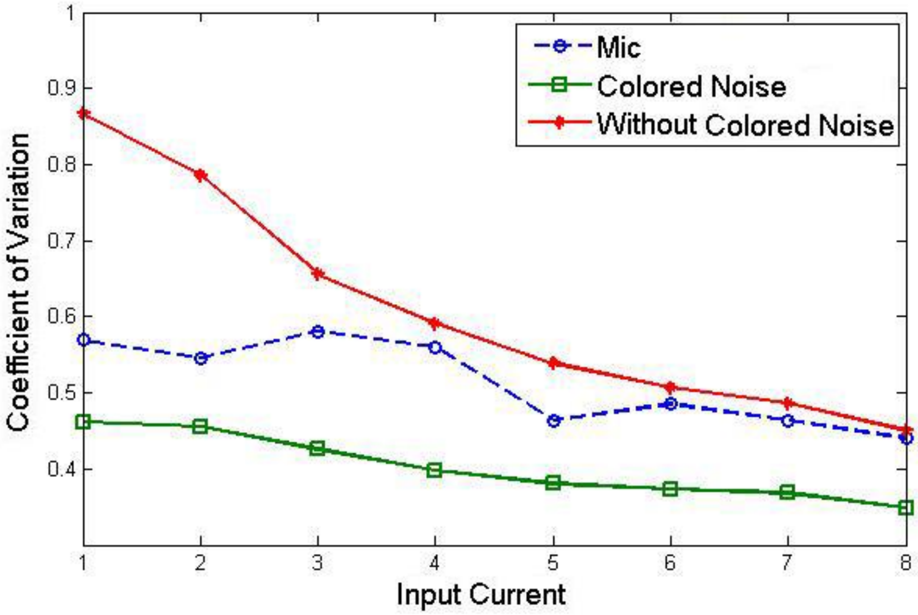

Figure 7: Coefficient of Variation for a Membrane of 600 Potassium and 2000 Sodium Channels. A 5 Sec. Time Was Used

In Figure above it appeared a special case that the without colored noise come closer to the microscopic simulation where the colored noise remain almost the same. The coherence of colored noise is still better than the without colored noise but the difference become smaller. In the small size membrane, the colored noise advantage remains regular.

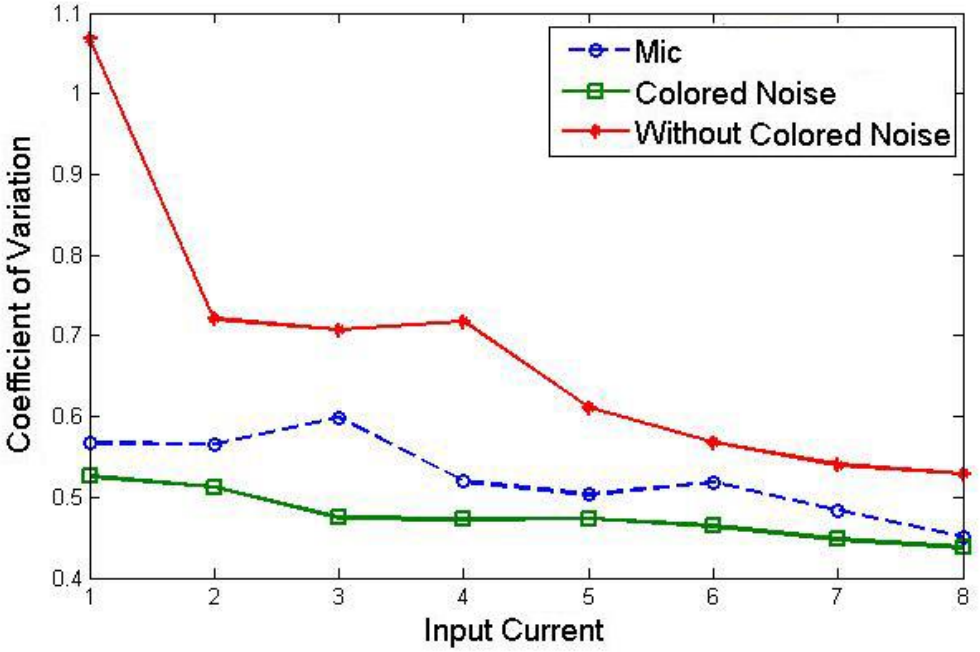

Figure 8: Coefficient of Variation for a Membrane of 1200 Potassium and 4000 Sodium Channels. A 5 Sec. Time Was Used

Enlarge the size of the cell membrane shows that the three plots start to get closer to each other and the difference between them become smaller as compare with the previous simulation. The difference in the coherence remains the same like the previous Figure.

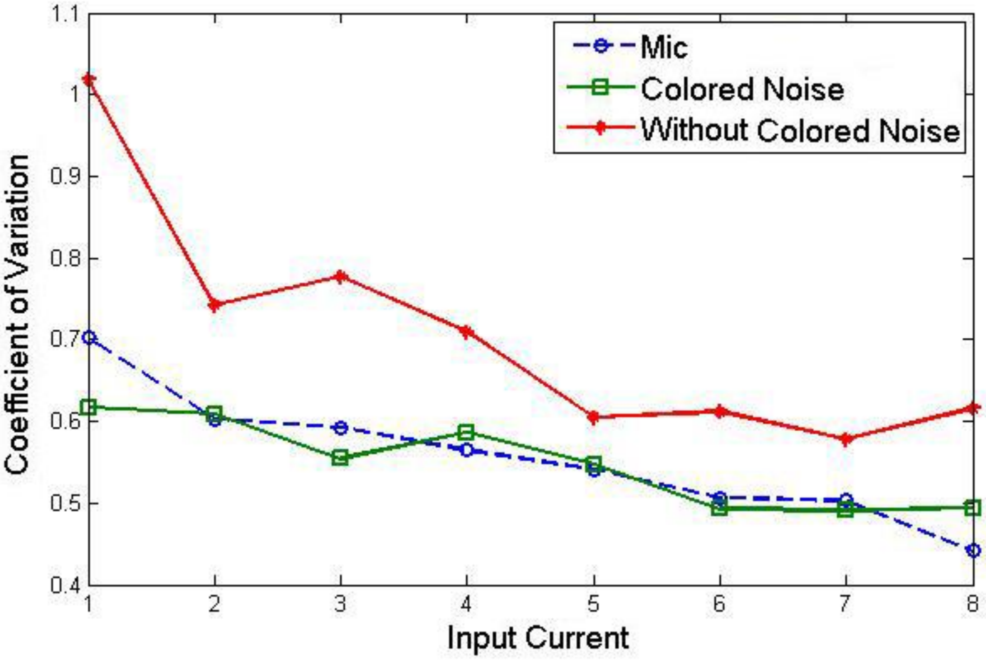

Figure 9: Coefficient of Variation for a Membrane of 1800 Potassium and 6000 Sodium Channels. A 5 Sec. Time Was Used

It can see after increasing the cell membrane size in the Figure 9 that the spike coherence in colored noise model is about at the same level as the coherence in the microscopic simulation scheme. But the spiking from without colored noise is less coherent as significantly larger coefficient of variation values are exhibited by the without colored noise spikes.

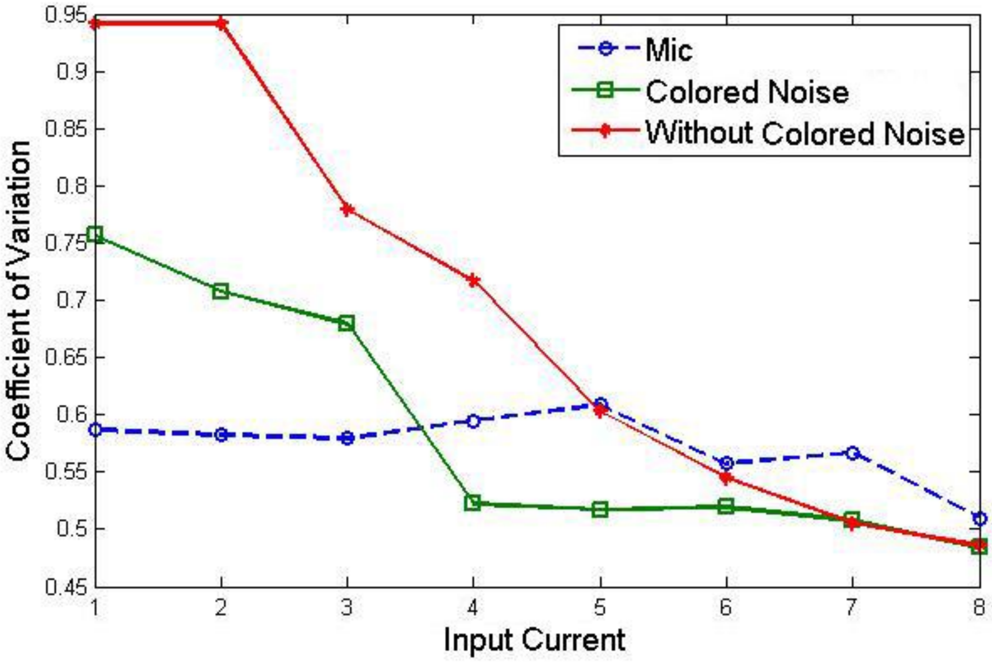

Figure 10: Coefficient of Variation for a Membrane of 3600 Potassium and 12000 Sodium Channels. A 5 Sec. Time Was Used

For large membrane size, the difference between three plots it become small and vanish when the input current is larger than 6 as shown in Figure above and the coherence of both the colored and without colored noise are at same level. From our experiments we suggest to use the colored noise term with small size membrane since it has low effectiveness on large size membrane.

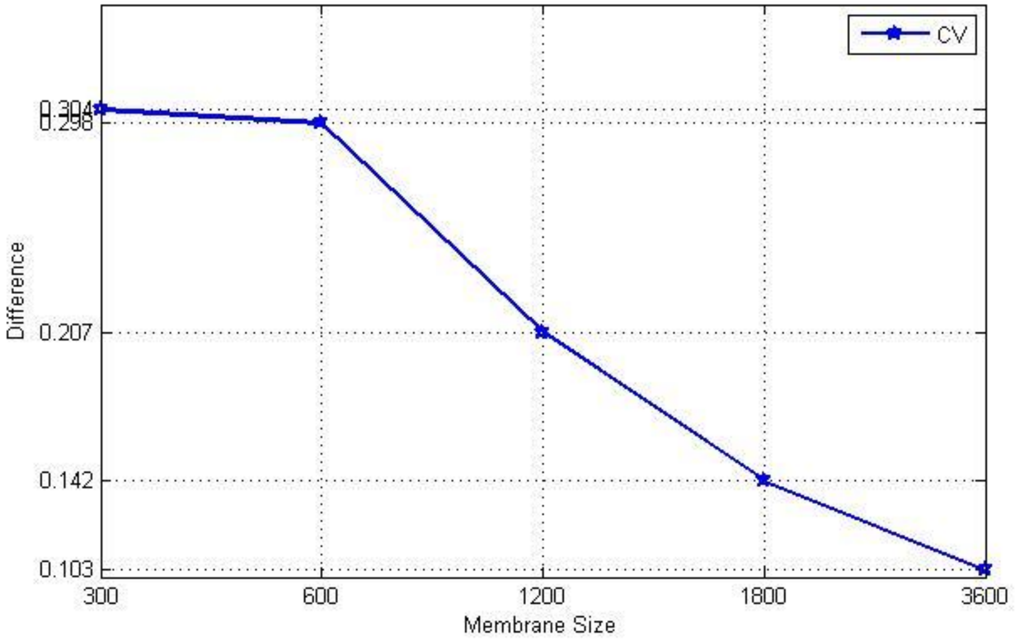

Figure 11: Difference Between $\boldsymbol{CV}$ of Colored Noise and $\boldsymbol{CV}$ of Colorless Through Whole Membrane Size

In this Figure we collect the values of coefficient of variation of both (the colored noise and without the colored noise) and subtract the first of the second and represent this values in the figure versus the membrane size of potassium channels for All previous experiments which shows the difference between them and as the membrane size start to increase the difference become smaller and vanish in last experiment.

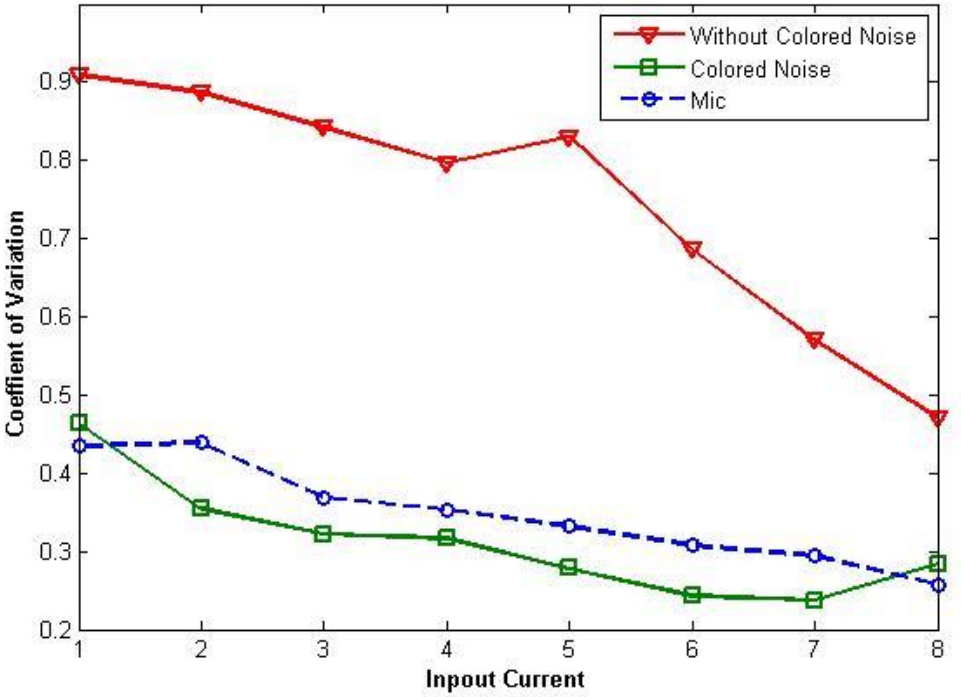

Figure 12: Coefficient of Variation for a Membrane of 600 Potassium and 1000 Sodium Channels. A 5 Sec. Time Was Used

The coefficient of variation versus the input current, the normal relationship between potassium channels and sodium channels is previous experiments is three multiples, but here we fixed the number of sodium channels to 1000 instead of 2000. We can see from the experiment the potassium channels and sodium are remained small. Therefore, the effect of colored noise is still the same and the result from without colored noise is remained far from microscopic simulation.

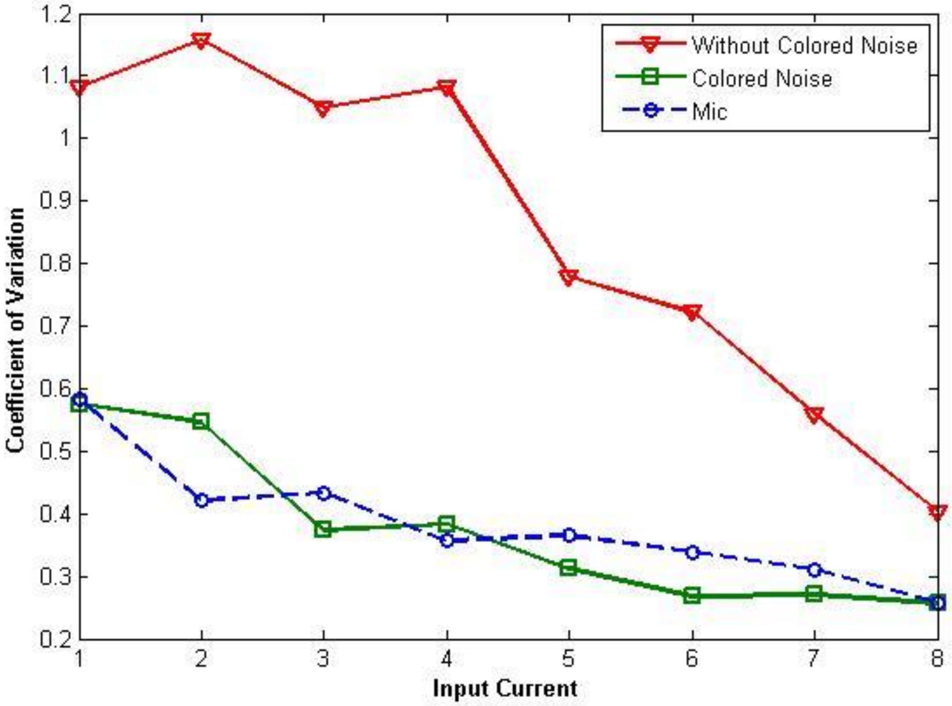

Figure 13: Coefficient of Variation for a Membrane of 3600 Potassium and 1000 Sodium Channels. A 5 Sec. Time Was Used

Increasing the number of potassium channels while the sodium is fixed will make the colored noise and microscopic noise very close to each other.

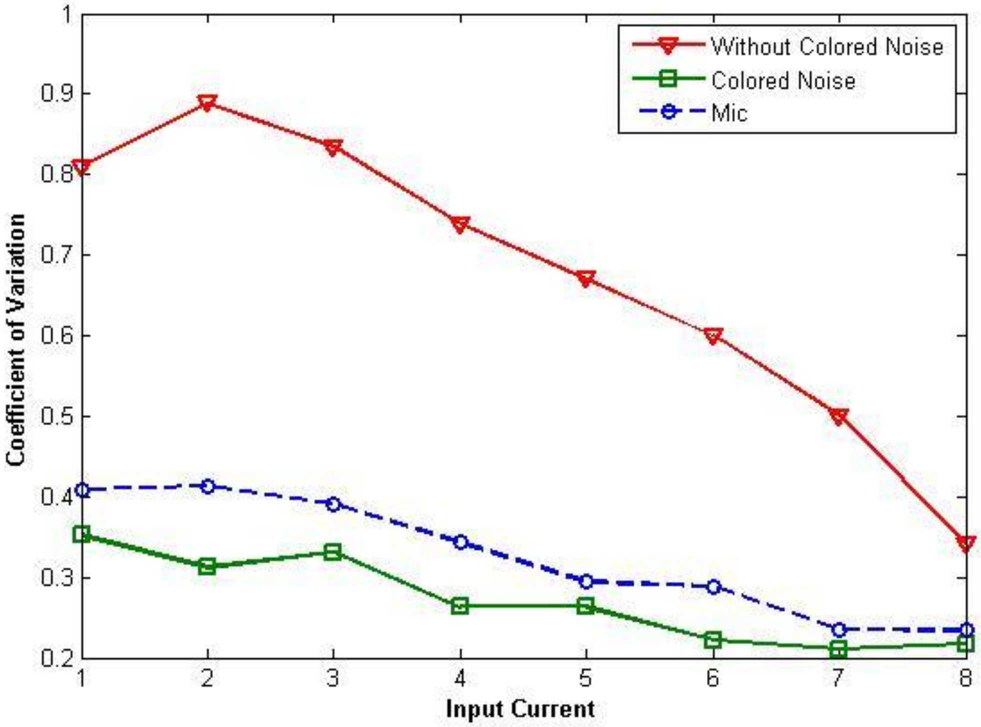

Figure 14: Coefficient of Variation for a Membrane of 600 Potassium and 4000 Sodium Channels. A 5 Sec. Time Was Used

The coefficient of variation against the input current, here we fixed the number of potassium channels to 600 and number of sodium channels to 4000 instead of 2000. Because the membrane area is small in this experiment the colored noise are near to microscopic and without far which shows fewer coherence of spike and exhibit a large coefficient of variation.

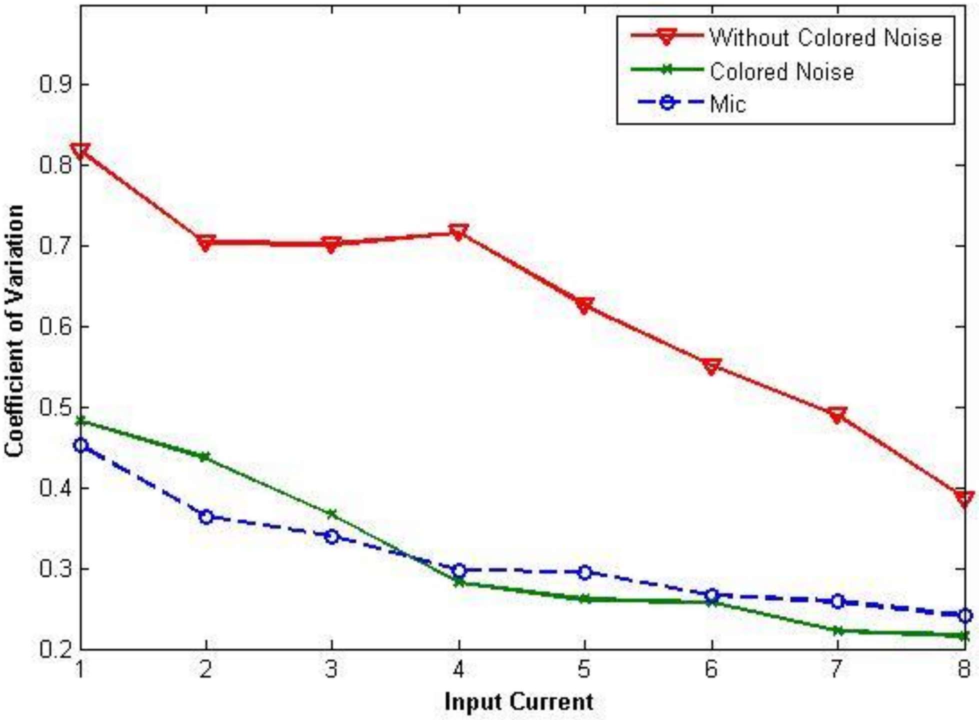

Figure 15: Coefficient of Variation for a Membrane of 600 Potassium and 12000 Sodium Channels. A 5 Sec. Time Was Used

In this Figure we increase the sodium channels to 12000 and the number of potassium channels is fixed, after we calculate the membrane area according to the number of channels ratio between sodium and potassium, the membrane size is consider small. So the result are still the same as before which is the colored noise and microscopic remains at same level that shows low CV and high coherence of spike train.

Chapter 7

CONCLUSION

In this thesis, statistics of the coefficient of variation was obtained from the colored stochastic model behavior, it was investigated by (Güler, 2013) when the membrane area is of limited size, and the voltage-gated ion channels accommodate a multiple number of gates individually. There, it was found that a non-trivially persistent correlation takes place between the fluctuations in the gating variables and the component of open channel fluctuations attributed to the gate multiplicity. This non-trivial phenomenon was found to be playing a main role for the elevation of excitability and spontaneous firing in small cells and enhance spike coherence significantly. Statistics of spike coherence from the articulated set of equations were found to be highly accurate in comparison with the corresponding statistics from the exact microscopic simulations, after extending stochastic Hodgkin-Huxley equations by incorporating colored noise terms into the conductances there to receive formalism capable of capturing the addressed cross correlations.

From our experiments results, the colored noise model investigate the phenomenon of the NCCP accurately, we observed that NCCP enhances the spike coherence. As mentioned before a way to measure the spike coherence is the coefficient of variation. In this thesis we examine the spike coherence through several experiments where it was measured by coefficient of variation given in equation (44). The coefficient of variation experiments executed for different membrane sizes. It seen that the CV for the colored noise model and the microscopic simulation scheme are at same level. However, the spiking from this model without colored noise is less coherence as appreciably larger coefficient of variation values displayed by without colored noise spikes. Therefore, in this work, we have compare between the coefficients of variation for a small membrane size to stochastic HH model using colored noise term, without colored noise and with microscopic simulation scheme. Also we have done experiments for a medium and large size. In small membrane size the without colored noise are far from the microscopic while colored noise are near to it. But when the membrane size for the same input current become larger these two terms come closer to the microscopic. Performance comparison shown that the increasing the membrane size and the value of input current in stochastic Hodgkin-Huxley equations with colored noise and without colored noise lead to the absence of difference between them. These mean that the effect of colored noise is vanished. The colored noise term depended on the membrane area whatever was the number of channels on it.

The recent study on this model was the coefficient of variation under input current. The input current is arguing with the colored noise. In future, investigating coefficient of variation using different type of noise, like white noise with input current to shed more light on the colored stochastic Hodgkin-Huxley equations.

REFERENCES

Abbott, L. F., & Dayan, P. (2002). *Theoretical Neuroscience: Computational and Mathematical Modeling of Neural Systems.* MIT press.

Bezrukov, S. &. (1995). *Noise-induced enhancement of signal transduction across voltage-dependent ion channels.* Nature, 378, 362–364.

Chow, C. C. (1996). *Spontaneous action potentials due to channel fluctuations.* Biophysical Journal, 71,3013–3021.

Clay, J. R., & DeFelice, L. J. (1983). *Relationship between membrane excitability and single channel open–closed kinetics.* Biophys. J.

DeFelice, L. J. (1992). *Chaotic states in a random world: Relationship between the nonlinear differential equations of excitability and the stochastic properties of ion channels.* Journal of Statistical Physics, 70, 339–354.

Diba, K. L. (2004). *Intrinsic noise in cultured hippocampal neurons: Experiment and modeling.* Journal of Neuroscience, 24, 9723–9733.

Dorval, A. D. (2005). *Channel noise is essential for perithreshold oscillations in entorhinal stellate neurons.* Journal of Neuroscience, 25, 10025–10028.

Faisal, A. A. (2007). *Stochastic simulations on the reliability of action potential propagation in thin axons.* PLoS Computational Biology, 3, e79.

Faisal, A. S. (2008). *Noise in the nervous system.* nervous system. Nature Reviews Neuroscience, 9, 292–303.

Güler, M. (2007). *Dissipative stochastic mechanics for capturing neuronal dynamics under the influence of ion channel noise: Formalism using a special membrane.* Physical Review E, 76,041918(17).

Güler, M. (2008). *Detailed numerical investigation of the dissipative stochastic mechanics based neuron model.* Journal of Computational Neuroscience, 25, 211–227.

Güler, M. (2011). *Persistent membranous cross correlations due to the multiplicity of gates in ion channels.* Journal of Computational Neuroscience ISSN 0929-5313.

Güler, M. (2013). Stochastic Hodgkin-huxley equations with colored noise terms in the conductances. *Neural Computation, 25, 46-74.*

Haberly L. B., O. c. (1990). The Synaptic Organization of Brain. In i. G. Haberly L. B. Olfactory cortex, *The Synaptic Organization of Brain* (pp. 317-345). New York: Oxford University.

Hille, B. (2001). *Ionic channels of excitable membranes (3rd ed.).* Massachusetts: Sinauer Associates.

Hodgkin, A. L. (1952). *A quantitative description of membrane current and its application to conduction and excitationin in nerve. Journal of Physiology.* (London.Print), 117, 500–544.

Izhikevich, E. M. (2007). *Dynamical Systems in Neuroscience:The Geometry of Excitability and Bursting.* San Diego, California.

Jacobson, G. A. (2005). *Subthreshold voltage noise of rat neocortical pyramidal neurones.* Journal of Physiology, 564,145–160.

Johansson, S. &. (1994). *Single-channel currents trigger action potentials in small cultured hippocampal neurons.* Proceedings of National Academy of Sciences USA, 91, 1761–1765.

Jung, P. &. (2001). *Optimal sizes of ion channel clusters.* Europhysics Letters, 56, 29–35.

Koch, C. (1999). *Biophysics of computation: Information processing in single neurons.* Oxford: Oxford University Press.

Kole, M. H. (2006). *Single Ih channels in pyramidal neuron dendrites: Properties, distribution, and impact on action potential output.* Journal of Neuroscience, 26, 1677–1687.

Lecar, H., & Nossal, R. (1971). I. Relationship between electrical noise and fluctuations in axon firing. In *Theory of threshold fluctuations in nerves* (p. 1048). Biophys. J.

Lu, F. R. (1994). Emergent collective behavior in large numbers of globally coupled independently stochastic ion channels.

Lynch, J. &. (1989). *Action potentials initiated by single channels opening in a small neuron (rat olfactory receptor).* Biophysical Journal, 55, 755–768.

Ochab-Marcinek, A. S. (2009). *Noise-assisted spike propagation in myelinated neurons.* Physical Review E, 79, 011904(7).

Özer, M. (2006). *Frequency-dependent information coding in neurons with stochastic ion channels for subthreshold periodic forcing.* Physics Letters A, 354, 258–263.

Rowat, P. F. (2004). *State-dependent effects of Na channel noise on neuronal burst generation.* Journal of Computational Neuroscience, 16, 87–112.

Rubinstein, J. (1995). *Threshold fluctuations in an N sodium channel model of the node of Ranvier.* Biophysical Journal,68, 779–785.

Sakmann, B. &. (1995). *Single-channel recording (2nded.).* New York: Plenum.

Schmid, G. G. (2001). *Stochastic resonance as a collective property of ion channel assemblies.* Europhysics Letters 56:22-28.

Schmid, G. G. (2003). *Channel noise and synchronization in excitable membranes.* Physica A 325, 165–175.

Schmid, G. G. (2004). *Effect of channel block on the spiking activity of excitable membranes in a stochastic Hodgkin–Huxley model.* Phys. Biol. 1, 61.

Schmid, G. H. (2007). *Intrinsic coherence resonance in excitable membrane patches.* Augsburg: Math Biosci 207:235-245.

Schneidman, E. F. (1998). *Ion channel stochasticity may be critical in determining the reliability and precision of spike timing.* Neural Computation, 10, 1679–1703.

Segev I., J. B. (2003). *Cable and compartment models of dendritic trees in bower.* the book of genesis 5:55.

Sigworth, F. J. (1980). *The variance of sodium current fluctuations at the node of Ranvier. Journal of Physiology.* (London Print), 307, 97–129.

Skaugen, E., & Walløe, L. (1979). *Firing behavior in a stochastic nerve membrane model based upon the Hodgkin–Huxley equations.* Acta Physiol. Scand.

Strassberg, A. F. (1993). *Limitations of the Hodgkin–Huxley formalism: Effects of single channel kinetics on transmembrane voltage dynamics.* Neural Computation 5, 843–855.

Whishaw, K. B. (2009). *Fundamental of Human Neuropsychology*. Worth Publishers.

Whishaw, K. B. (2012). *Fundamentals of Human Physiology FOURTH EDITION.* Virginia United States.

White, J. A., Klink, R., Alonso, A., & Kay, A. R. (1998). *Noise from voltage-gated ion channels may influence neuronal dynamics in the entorhinal cortex.* Journal of Neurohysiology, 80, 262–269.

White, J. A., Rubinstein, J. T., & Kay, A. R. (2000). Channel noise in neurons. *Trends Neurosci.*, 23, 131–137.

Zeng, S. &. (2004). Mechanism for neuronal spike generation by small and large ion channel clusters. *Physical Review E, 70, 011903(8).*

Zwanzig, R. (2001). *Non-equilibrium statistical mechanics.* Oxford University.